MRI of Brain Disease in Veterinary Patients Part 2: Acquired Brain Disorders

Silke Hecht, Dr Med Vet*, William H. Adams, DVM

KEYWORDS

• Magnetic resonance imaging • Cat • Dog • Neoplasia
• Inflammation • Infarct

INFLAMMATORY BRAIN DISEASES

Inflammatory brain diseases can affect brain parenchyma (encephalitis), meninges (meningitis), or both (meningoencephalitis).[1] Depending on the underlying causes, involvement of the spinal cord (myelitis/meningomyelitis) may occur. Encephalitis may cause no detectable abnormalities on magnetic resonance imaging (MRI), or may manifest as multifocal (rather than focal or diffuse) lesions associated with brain parenchyma that typically appear hyperintense on T2-weighted (T2-W) images, and hypointense on T1-weighted (T1-W) images.[2–4] Fluid attenuated inversion recovery (FLAIR) has higher sensitivity than conventional spin-echo sequences in detecting subtle brain lesions in dogs with clinical signs of multifocal brain disease, and its use is encouraged in all of these cases.[5] Meningitis may not be detected with MRI, or may appear as meningeal enhancement following administration of contrast medium.[2–4,6]

Infectious Inflammatory Brain Diseases

Canine distemper virus (CDV) and feline infectious peritonitis virus (FIPV) are the most common causes of viral encephalitis in dogs and cats, respectively. In acute CDV infection, T2 hyperintense lesions, and loss of contrast between gray and white matter on T2-W images, may be found in cerebellum or brainstem, corresponding to areas of demyelination.[7] T2 hyperintense areas are occasionally seen in the temporal lobes, which may be related to infection or postictal edema. MRI findings in chronic distemper meningoencephalitis include essentially bilaterally symmetric T2 hyperintensity of the cortical gray/white matter junction of the parietal and frontal lobes, T2

Department of Small Animal Clinical Sciences, University of Tennessee College of Veterinary Medicine, 2407 River Drive, Knoxville, TN 37996, USA
* Corresponding author.
E-mail address: shecht@utk.edu (S. Hecht).

Vet Clin Small Anim 40 (2010) 39–63
doi:10.1016/j.cvsm.2009.09.006 **vetsmall.theclinics.com**
0195-5616/09/$ – see front matter

hyperintensity of the arbor vitae of the cerebellum with partial loss of cerebellar cortical gray/white matter demarcation, subtle focal T2 hyperintensity of the pons, and meningeal contrast enhancement.[8] In feline infectious peritonitis (FIP), MRI may show T2 hyperintensity and contrast enhancement of ventricular lining, choroid plexus and meninges compatible with ependymitis, choroiditis, and meningitis (**Fig. 1**).[1,4,9] Concurrent hydrocephalus is common, and herniation of the cerebellum secondary to increased intracranial pressure is possible.[4]

Mechanisms of bacterial infection of the central nervous system (CNS) in cats and dogs include hematogenous spread, contiguous infection from adjacent structures (inner ears, cribriform plate, sinuses, eyes, and vertebrae), direct inoculation (trauma, bite wound, and surgery), and migration of foreign bodies or aberrant parasites. In addition to meningitis (**Fig. 2**) and meningoencephalomyelitis, CNS infection may result in focal parenchymal abscesses or empyema in subdural or epidural locations.[10] MRI features of intracranial infection secondary to plant foreign-body migration,[11] due to hematogenous spread from a mediastinal abscess,[12] secondary to bacterial endocarditis,[13] secondary to local extension from a retrobulbar abscess,[14] and as complication of otitis media or interna,[15] have been described. Intracranial abscesses are typically hypointense on T1-W and hyperintense on T2-W images, with strong peripheral contrast enhancement and associated brain edema. Concurrent meningitis appearing as meningeal enhancement is common. Presumed rupture of an abscess into the ventricular system in a dog resulted in failure of cerebrospinal fluid (CSF) to suppress on FLAIR.[16]

Fungal infections have been reported to affect the CNS, with varied MRI findings.[17] Imaging findings in cats with CNS cryptococcosis include solitary or multifocal mass lesions that are typically hyperintense on T2-W images and show variable degrees of contrast enhancement. Diffuse and patchy meningeal, ependymal, and choroid plexus enhancement are also possible.[17–19] In dogs with cryptococcosis, T1 hypointense and T2 hyperintense lesions with multifocal (ring) enhancement and meningeal enhancement have been reported.[17,20,21] Extension of a cryptococcal fungal granuloma through the cribriform plate was observed in 1 dog.[17] *Cladophialophora bantiana* meningoencephalitis appeared as an irregularly shaped area of increased T2 signal intensity and

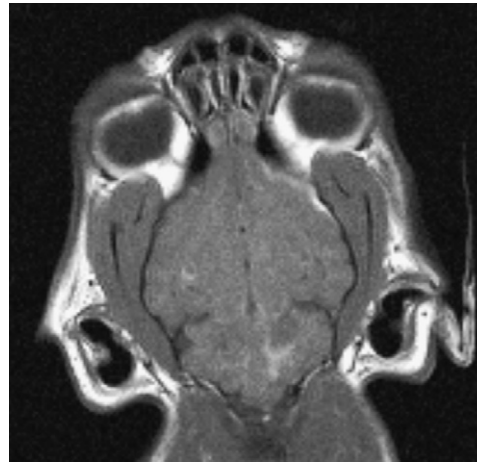

Fig. 1. Dorsal T1-W postcontrast image of a 2-year-old cat with presumptive diagnosis of FIP. There is contrast enhancement associated with meninges and ventricular lining, consistent with meningitis and ependymitis.

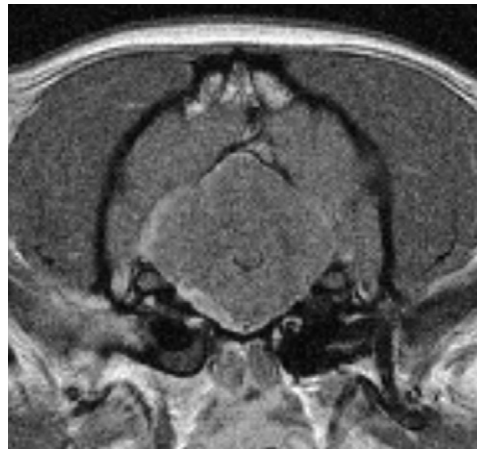

Fig. 2. Meningitis in a 5-year-old pug secondary to otitis media. On transverse T1-W post-contrast image, extensive enhancement and thickening of the meninges of the right cerebellum and brainstem are noted, along with enhancement of the external ear canal. Low-signal material within the right tympanic bulla does not show evidence of contrast enhancement consistent with exudate.

mass effect in the cerebral white matter of the parietal and temporal lobes of a dog, with nonuniform contrast enhancement of mass and meninges observed on postcontrast images.[22] The same organism in a cat appeared as a large uniformly contrast-enhancing mass involving the cerebellum and pons.[23] MRI findings in a cat with histoplasmosis included a single high-signal T2/low-signal T1 uniformly contrast-enhancing intra-axial mass of the frontal lobe with severe concurrent edema.[23]

Parasitic meningoencephalitis in dogs and cats is caused by aberrant migration of parasites such as *Dirofilaria*, *Baylisascaris*, *Cuterebra*, *Taenia*, *Ancylostoma*, *Toxascaris* and *Angiostronglylus*.[24] MRI features include focal or multifocal parenchymal lesions of variable signal intensity, and peripheral parenchymal or meningeal contrast enhancement.[21,25–27] Intraparenchymal hemorrhage is a common feature in parasite migration, and T2*-W images are useful in establishing a presumptive diagnosis.

Protozoal meningoencephalitis may be caused by *Toxoplasma* and *Neospora* infection in dogs and *Toxoplasma* infection in cats.[24] MRI in a dog with neosporosis demonstrated T2 hyperintensity of the vermis and cerebellar hemispheres with subtle contrast enhancement.[21] CNS toxoplasmosis in cats appeared as multifocal, indistinct, contrast-enhancing parenchymal lesions which were iso- to hypointense on T1-W images, hyperintense on T2-W images, and were associated with edema.[4]

Noninfectious Inflammatory Brain Diseases

Several inflammatory conditions unrelated to infectious agents have been identified in several different canine breeds.[28]

Granulomatous meningoencephalitis (GME) is an inflammatory CNS disorder of uncertain cause that can affect any breed but most often occurs in young to middle-aged toy-breed dogs.[29] The disease can affect the brain or spinal cord. On MRI, GME lesions can be focal or multifocal, and commonly affect the brain stem. Although the disease has a predilection for white matter, it is not associated with distinct topography.[28] Lesions are typically hyperintense on T2-W and FLAIR images, iso- to hypointense on T1-W images, and variably contrast-enhancing, ranging from

none to intense contrast uptake (**Fig. 3**).[30–32] Meningeal enhancement may[6] or may not[30] be observed.

Necrotizing meningoencephalitis (NME) is of uncertain cause and is characterized by cavitary necrosis in the neuroparenchyma. The disease was initially described in the pug breed (''pug dog encephalitis''),[33] but similar disorders have since been reported in other small breeds, including the Maltese,[34] Chihuahua,[35] Pekingese,[36] French bulldog,[37] Shi Tzu,[28] and Lhasa apso.[28] A distinct form of NME, described mainly in Yorkshire terriers, has been termed necrotizing leukoencephalitis (NLE).[28] Descriptions of imaging findings in this group of inflammatory brain disorders are not available for all breeds affected, but there seem to be breed-specific differences.[38] In almost all cases of NLE reported in Yorkshire terriers, lesions were found to be associated with the cerebrum and brainstem. On magnetic resonance (MR) images, these lesions appear iso- to hypointense on T1-W images, hyperintense on T2-W and FLAIR images, and show variable contrast enhancement.[28,39–42] Concurrent hydrocephalus of variable severity is possible. Unlike NLE, NME in pugs usually does not involve the cerebellum, brainstem, or spinal cord. MRI findings include diffuse asymmetric lesions restricted to the forebrain, affecting both cerebral hemispheres.[28,38,43] Lesions are nonuniformly hyperintense on T2-W, isointense to hypointense on T1-W images, and affect gray and white matter, resulting in loss of gray/white matter distinction (**Fig. 4**). Additional MRI findings include variable degrees of contrast enhancement of brain and meninges, asymmetry of lateral ventricles, brain herniation, and T2/FLAIR hyperintensity associated with hippocampus and piriform lobes. MRI of the brain in 2 Chihuahuas with NME demonstrated multifocal loss of cortical gray/white matter demarcation with hypointensity on T1-W, hyperintensity on T2-W/FLAIR images, and slight contrast enhancement.[35] In 1 dog there was involvement of the medulla, and asymmetric hydrocephalus was noted in the second animal. A French bulldog had asymmetry of both lateral ventricles, cerebrum, midbrain, and several distinct T2 hyperintense white matter foci of the forebrain and the brain stem, with variable contrast enhancement.[37]

Other Inflammatory Intracranial Diseases

Idiopathic eosinophilic meningitis/meningoencephalitis in dogs may not show abnormalities on MRI, or may have variable findings including patchy regions of T2

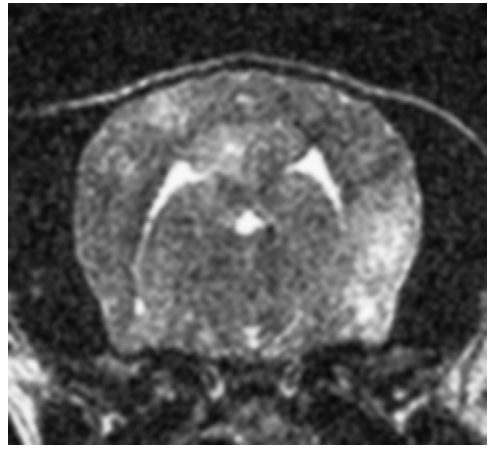

Fig. 3. Granulomatous meningoencephalitis in a 2-year-old toy poodle. On transverse T2-W image, multifocal hyperintense lesions are associated with both cerebral hemispheres.

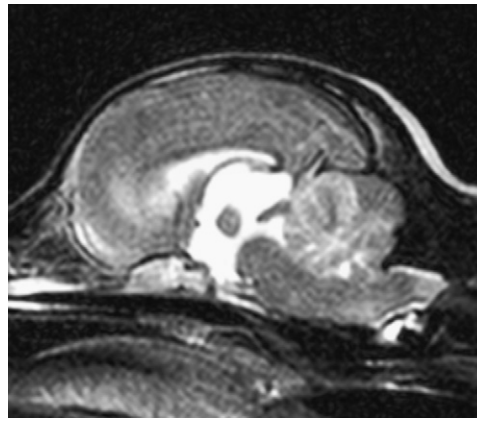

Fig. 4. NME in an 8-year-old Maltese. Sagittal T2-W image demonstrates multiple poorly circumscribed hyperintense lesions within the cerebrum, cerebellum, brainstem, and spinal cord.

hyperintensity and contrast enhancement in the cerebral cortex, solitary or multiple masses, meningeal enhancement, and enlargement and contrast enhancement of cranial nerves.[21] A case of lymphocytic meningoencephalitis in a cat was characterized by focal T1 isointense and T2 hyperintense contrast-enhancing lesions.[4] No intracranial abnormalities were detected on MRI in a cat with histiocytic encephalitis.[4] Trigeminal neuritis in dogs is characterized by diffuse enlargement of the nerve without a mass lesion. Affected nerves are isointense to brain parenchyma on T1-W and PD-W images, isointense or hyperintense on T2-W images, and show contrast enhancement.[44]

CEREBROVASCULAR DISEASE

The term ''cerebrovascular diseases'' refers to all disorders in which there is an area of brain transiently or permanently affected by ischemia or bleeding, or in which 1 or more blood vessels of the brain are primarily impaired by a pathologic process.[45]

Intracranial Aneurysms and Cerebrovascular Malformations

An aneurysm is an abnormal focal enlargement of an artery of variable cause.[46] Patent aneurysms appear as signal void on T1-W and T2-W images, representing fast flowing blood. Small aneurysms, and aneurysms with turbulent flow, are unreliably shown on conventional MRI, and are better demonstrated by magnetic resonance angiography (MRA).[46,47] A case of a presumed aneurysm, most likely the result of traumatic arteriovenous fistulization, has been described in a dog.[48] On computerized tomography (CT) images, an expansile enhancing mass was present along the intracranial cavernous sinus and extended through the orbital fissure into the retrobulbar space. With MRI, the structure appeared as a signal void due to the presence of rapidly flowing blood. The vascular origin of the lesion was confirmed with MRA.

Cerebrovascular malformations are congenital anomalies of brain vasculature.[49] Different types include arteriovenous malformations (clusters of abnormal arteries and veins with direct arterial-to-venous shunts), venous malformations (anomalous veins separated by normal neural parenchyma), cavernous malformations (masses of contiguous sinusoidal vessels with no intervening parenchyma), and telangiectasias (masses of small capillary-type vessels separated by normal parenchyma). Animals

with cerebrovascular abnormalities usually present with intracranial hemorrhage, and imaging findings are consistent with hemorrhagic stroke (see later).[1,39] Identification of associated large vessels suggests vascular malformation as the underlying cause of spontaneous intracranial hemorrhage. However, compression or obliteration of vessels by hematoma, extremely slow flow, and thrombosis may obscure the abnormal vessels, and specialized techniques (catheter angiography, repeat MRI or MRA) may be needed to achieve a diagnosis.[46]

Stroke (Cerebrovascular Accident, Infarct)

A stroke is a suddenly developing focal neurologic deficit resulting from an intracranial vascular event.[50] In ischemic stroke, blood flow to an area of tissue is compromised due to intracranial arterial or venous obstruction. Hemorrhagic stroke results from rupture of intracranial blood vessels.

Ischemic strokes can be categorized according to anatomic site, size, age, type (pallid or hemorrhagic), pathology (arterial vs venous), mechanism (thrombotic, embolic, hemodynamic), and etiology.[45] Causes of ischemic stroke in dogs include atherosclerosis associated with primary hypothyroidism,[51] hypertension and diabetes,[52] embolic metastatic tumor cells,[51] chronic renal disease,[51–53] hyperadrenocorticism,[51,53] intravascular lymphoma,[54,55] septic thromboemboli,[56] fibrocartilaginous embolism,[57] migrating parasite or parasitic emboli (*Dirofilaria immitis*),[58] and a hypercoagulable state associated with hyperadrenocorticism, protein losing nephropathy (PLN), or neoplasia.[53] In approximately 50% of dogs with ischemic stroke, no underlying medical condition is identified.[53] Territorial infarcts occur when one of the main arteries supplying the brain is occluded. Lacunar infarcts are defined as subcortical infarcts limited to the vascular territory of an intraparenchymal superficial or deep perforating artery.[59] Small-breed dogs are more likely to have territorial cerebellar infarcts, and large-breed dogs are more likely to have lacunar thalamic or midbrain infarcts.[53] Cavalier King Charles spaniels and greyhounds may be predisposed for infarcts.[53,60] Watershed infarcts, defined as infarcts in the boundary zone between large artery territories,[59] do not seem to be common in veterinary patients.[53] Diffusion weighted imaging (DWI) is sensitive to alterations in brain parenchyma following stroke, and is capable of demonstrating abnormalities within minutes of an event.[61] Restricted diffusion (impairment of normal Brownian motion) occurs secondary to failure of the cell membrane ion pump and subsequent cytotoxic edema. This appears as marked hyperintensity on DWI, and hypointensity on a synthesized apparent diffusion coefficient (ADC) map derived from 2 or more DWI.[62] On conventional MRI sequences, changes will be apparent within 12 to 24 hours of onset. Although MRI findings in ischemic stroke may be similar to changes seen with other brain parenchymal diseases, certain distinguishing characteristics exist (**Fig. 5**).[52,53,60,63–65] An ischemic infarct appears as a homogeneous T2 hyperintense area with sharp demarcation between affected and nonaffected parenchyma, and minimal to no mass effect. Lesions are typically confined to gray matter, but may involve white matter in severe cases.[65] Faint diffuse or peripheral contrast enhancement may be noted and has been reported in patients imaged between 1 and 45 days postonset of neurologic signs.[60] Reperfusion injury of an ischemic infarct can occur, resulting in hemorrhagic infarction.[59]

Hemorrhagic stroke can be classified according to anatomic site (intraparenchymal, epidural, subdural, subarachnoid, and intraventricular), size, age, and cause (eg, intracranial neoplasia,[66] von Willebrand factor deficiency[67] and other coagulopathies, parasite migration,[25,27] cerebral vascular malformation,[39] idiopathic). The appearance of hemorrhage on MRI changes over time, allowing staging of a hematoma using conventional MRI sequences (**Table 1**).[68,69] However, there is considerable variability

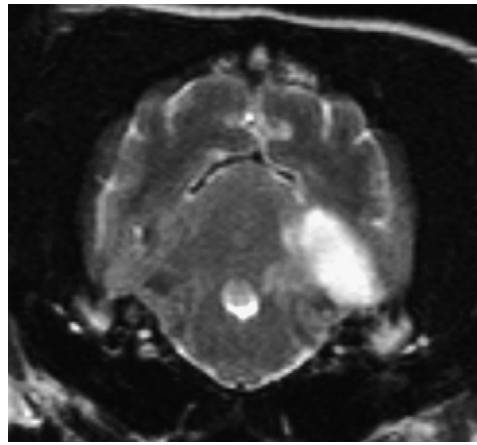

Fig. 5. Transverse T2-W image of the caudal fossa in a dog, demonstrating a wedge-shaped hyperintensity associated with the left cerebellar hemisphere consistent with an ischemic infarct.

in the appearance of hemorrhage on MRI. Hemorrhage in areas with high ambient oxygen (ventricles; epidural, subdural, and subarachnoid space) "ages" more slowly than parenchymal or neoplastic hematomas, with a resultant change in time course of degradation.[68] Deoxyhemoglobin, intracellular methemoglobin, hemosiderin, and ferritin have high magnetic susceptibility and are depicted with high sensitivity on T2*-W images (**Fig. 6**A).[70] Intraparenchymal hemorrhage appears as mass lesion(s) of variable size and intensity,[71] and (sub)acute parenchymal hemorrhage is often associated with brain edema. In the acute stage, there is no contrast enhancement of the hematoma. However, with time, neovascularization in the surrounding brain tissue develops, resulting in ring enhancement of the lesion.[69] Identification of underlying cause of intraparenchymal hemorrhage can be challenging. The signal of hematomas secondary to neoplasms is more heterogeneous and complex than in spontaneous hematomas because of the presence of hemorrhagic components of varied age and, therefore, hemoglobin state, presence of nonhemorrhagic areas,

Table 1
Change of appearance of intracranial hemorrhage over time

Stage	Time Frame	Hemoglobin State	Intensity (T1-W)	Intensity (T2-W)
Hyperacute	<12–24 h	Intracellular oxyhemoglobin	Isointense or hypointense	Hyperintense
Acute	1–3 d	Intracellular deoxyhemoglobin	Isointense or hypointense	Hypointense
Early subacute	>3 d	Intracellular methemoglobin	Hyperintense	Hypointense
Late subacute	>7 d	Extracellular methemoglobin	Hyperintense	Hyperintense
Chronic	>14 d	Hemosiderin and ferritin	Hypointense	Hypointense

Data from Bradley Jr WG. MR appearance of hemorrhage in the brain. Radiology 1993;189(1):15–26 and Parizel PM, Makkat S, Van Miert E, et al. Intracranial hemorrhage: principles of CT and MRI interpretation. Eur Radiol 2001;11(9):1770–83.

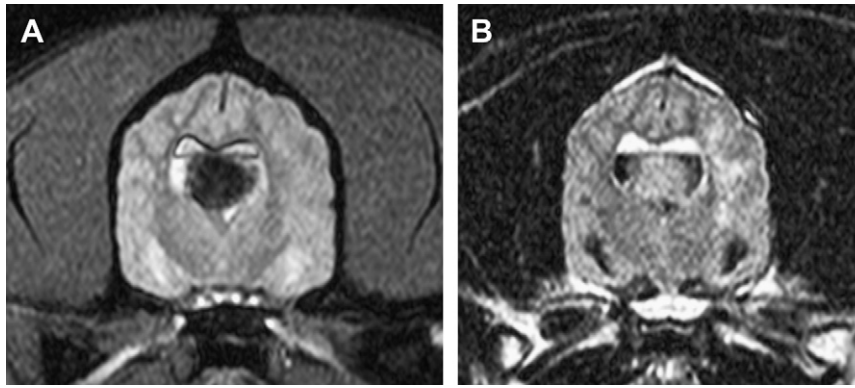

Fig. 6. Acute hemorrhagic stroke of undetermined cause in an 8-year-old boxer. The dog was positioned in dorsal recumbency for the examination. On T2*-W image (*A*) a large interventricular susceptibility artifact, consistent with hemorrhage, is noted. On FLAIR image (*B*) a fluid-fluid level between hypointense CSF and hyperintense CSF/blood mixture in the dependent part of the ventricles is noted.

and, in some instances, presence of necrotic-cystic components.[72] Epidural hemorrhage assumes a focal biconvex configuration that may cross dural folds, such as falx and tentorium, but not sutures, whereas subdural hemorrhage appears as a peripheral crescent-shaped collection of blood that may cross suture lines but is limited by the falx cerebri and tentorium cerebelli.[1,68,69] Subarachnoid and intraventricular hemorrhages result in admixture of blood and CSF. If massive bleeding has occurred, separation of intraventricular fluid into hemorrhagic and nonhemorrhagic strata may be observed (**Fig. 6**B). Subarachnoid or intraventricular thrombus may be present.[68]

Other Vascular Disorders

Feline ischemic encephalopathy (FIE) is a syndrome of cerebral infarction affecting adult cats, which is attributed to aberrant *Cuterebra* spp larval migration in the brain and toxin release by the parasites.[50,73] MRI findings in chronic FIE include asymmetry of the cerebral hemispheres and bilateral symmetric enlargement of the subarachnoid space over the temporal lobes in areas supplied by the middle cerebral artery.[74] MRI-detectable histopathologic lesions include parasitic tracks, superficial laminar cerebrocortical necrosis, cerebral infarction, subependymal rarefaction and astrogliosis, and subpial astrogliosis.[73]

In global brain ischemia (GBI) the entire brain is affected by a transient period of complete ischemia, followed by reperfusion.[75] MRI findings include bilaterally symmetric increased T2/FLAIR signal intensity associated with gray matter and, to a lesser degree, with white matter of the occipital and parietal lobes and caudate nuclei/thalamus.[76,77] Bilaterally symmetric contrast enhancement in these areas may be observed.[77] In a report of a dog with GBI, repeat examination showed that lesions associated with gray matter decreased in extent and severity, and white matter changes resolved.[76]

METABOLIC, NUTRITIONAL, TOXIC, AND DEGENERATIVE ENCEPHALOPATHIES

Lysosomal storage diseases comprise a wide variety of inherited abnormalities that are characterized by the intracellular accumulation of 1 or more products of an

interrupted degradative metabolic pathway.[24] Globoid cell leukodystrophy (Krabbe disease) is caused by mutations in the gene for galactocerebrosidase, and has been described in cairn terriers and west highland white terriers.[78] MRI findings include mild hydrocephalus, increased signal intensity in the corpus callosum on T1-W images, bilaterally symmetric increased signal intensity of the corpus callosum, centrum semiovale, internal capsule, corona radiata and cerebellar white matter on T2-W images, and symmetric enhancement of the corpus callosum, internal capsule, and corona radiata after administration of gadolinium.[79] Gangliosidoses are characterized by excessive neuronal accumulation of ganglioside. MRI findings have been reported in a golden retriever with G_{M2}-gangliosidoses and included mild cerebral atrophy and bilaterally symmetric T2 hyperintensity and T1 hypointensity to the caudate nucleus without evidence of contrast enhancement.[80] MRI examinations performed on 2 canine mutants with G_{M1} gangliosidosis (English springer spaniel and Portuguese water dog) demonstrated a relative increase in gray matter and an abnormal signal intensity of cerebral and cerebellar white matter on T2-W images.[81] Ceroid lipofuscinosis is characterized by the abnormal accumulation of lipoprotein pigment within cellular lysosomes. MRI findings include dilation of cerebral sulci and cerebellar fissures and ventriculomegaly.[82,83] In cats affected with α-mannosidosis, a decrease in ADC values of white and gray matter and an increase in T2 values of white matter have been reported, corresponding to neuronal swelling, abnormal myelin, and astrogliosis.[84,85] Mucopolysaccharidoses (MPS) are a group of diseases caused by different specific deficits of metabolism of glycosaminoglycan. No abnormalities were detected on MRI examination of the brain in schipperkes with MPS III.[86]

L-2-Hydroxyglutaric aciduria is an inborn error of metabolism that has been described in Staffordshire bull terriers.[87] MRI findings included bilaterally symmetric, diffuse regions of gray matter hyperintensity on T2-W images, and T1-W hypointensity most prominent in the thalamus, hypothalamus, dentate nucleus, basal ganglia, dorsal brainstem, cerebellar nuclei, and cerebellar gyri. These lesions did not exhibit a mass effect and did not show evidence of contrast enhancement.

Mitochondrial encephalopathies resembling subacute necrotizing encephalomyelopathy (Leigh syndrome) in humans have been described in Australian cattle dogs[88] and Alaskan Huskies,[89,90] and similar diseases have been suspected in English springer spaniels, Yorkshire terriers, and cats.[24] MRI findings in hereditary polioencephalomyelopathy in an Australian cattle dog included bilaterally symmetric abnormalities in areas corresponding to the interposital nuclei in the cerebellum and the vestibular nuclei in the medulla, and in areas corresponding to the dorsal nuclei of the trapezoid body, pontine nuclei, caudal colliculi, and the dorsolateral reticular formation.[91] Lesions were isointense or hypointense on T1-W images, hyperintense on T2-W images, did not have a mass effect, and did not show evidence of contrast enhancement. MRI examination in an Alaskan husky with subacute necrotizing encephalopathy revealed bilateral cavitation extending from the thalamus to the medulla, with less-pronounced degenerative lesions in the caudate nucleus, putamen, and claustrum.[90]

Failure of the liver to remove toxic substances absorbed from the gastrointestinal tract may result in hepatic encephalopathy.[24] MRI findings in dogs and cats with congenital portosystemic shunt include brain atrophy, possibly unrelated to shunt, and bilaterally symmetric hyperintensity to the lentiform nuclei on T1-W images without contrast enhancement.[92]

Thiamine deficiency results in insufficient adenosine triphosphate (ATP) production in the brain, with subsequent neuronal dysfunction.[24] MRI findings in dogs include bilaterally symmetric multifocal T2, FLAIR, and postcontrast T1 hyperintensities in the red nuclei, caudal colliculi, vestibular nuclei of the brainstem, and the cerebellar

nodulus,[93] or bilaterally symmetric T2 hyperintensities in caudate nuclei and rostral colliculi.[94] In cats, bilaterally symmetric T2, FLAIR, and T2* hyperintense nonenhancing lesions are observed associated with the lateral geniculate nuclei, caudal colliculi, periaqueductal gray matter, medial vestibular nuclei, cerebellar nodulus, and facial nuclei (**Fig. 7**),[95] with the caudal colliculi, medial vestibular nuclei, and facial nuclei also being hyperintense on T1-W images.

Myelinolysis is a brain disorder most commonly caused by rapid correction of hyponatremia in humans, but probably multifactorial.[96] Lesions were originally believed to be limited to the pons, but extrapontine locations including the thalamus, midbrain, cerebellum, basal nuclei, and cerebrocortical gray and white matter junctions have been reported. MRI findings in dogs include bilaterally symmetric T2/FLAIR hyperintense nonenhancing lesions within the thalamus,[97] caudate nuclei, and along the cerebrocortical gray-white matter junction.

A series of progressive neurologic diseases have been summarized under the term ''spongy degeneration.''[50] These conditions are primarily, but not exclusively, diseases of white matter, and may be hereditary. MRI findings in spongy degeneration of the CNS in a Labrador retriever included large, bilaterally symmetric T2 hyperintense and T1 hypointense nonenhancing lesions in the region of the deep cerebellar nuclei, and smaller lesions within the thalamus ventromedial to the lateral ventricles.[98]

Neuroaxonal dystrophy is a degenerative disease of the CNS characterized by degeneration of neurons and axons. MRI features in a papillon included cerebral and cerebellar atrophy.[99]

Cerebellar cortical abiotrophy refers to the degeneration of normal neuronal cell populations within the cerebellar cortex after birth, and has been reported in a variety of breeds.[50] Presumptive diagnosis is best made on sagittal T2-W images, in which the small size of the cerebellum is indicated by a marked increase in fluid separating the folia of the cerebellum (**Fig. 8**).[100–104] Differentiation of true abiotrophy from other causes of small cerebellar size (cerebellar atrophy, cerebellar hypoplasia) is not possible based on imaging findings.

TRAUMA

MRI findings in head trauma in dogs and cats are infrequently reported. Possible findings include fractures,[74,105] intracranial hemorrhage,[106,107] brain edema,[105] and

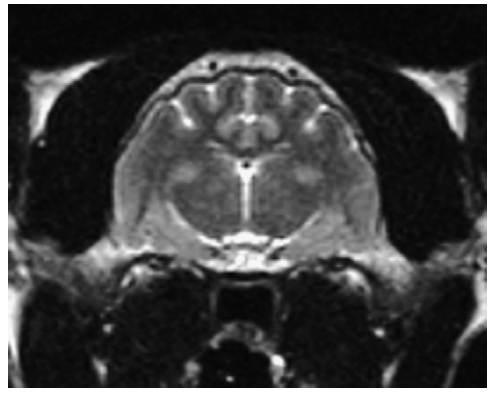

Fig. 7. Presumptive thiamine deficiency in a 7-year-old cat. On transverse T2-W image, there are bilaterally symmetric T2 hyperintense lesions associated with the thalamus, corresponding to the location of the lateral geniculate nuclei.

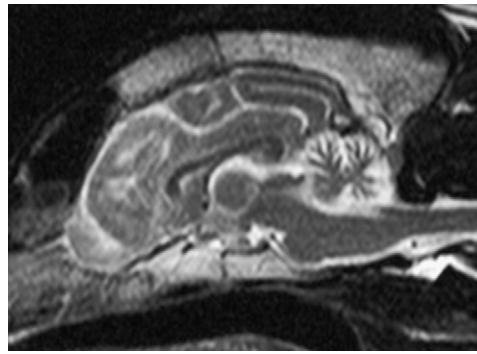

Fig. 8. Cerebellar abiotrophy in a 6-year-old Staffordshire terrier. Sagittal T2-W image demonstrates the small size of the cerebellum, indicated by increase in fluid separating the folia of the cerebellum.

parenchymal brain defects with compensatory CSF filling (hydrocephalus ex vacuo) (**Fig. 9**).[74] MRI appearance of traumatic intracranial hemorrhage corresponds to imaging features described earlier (see section on Stroke (Cerebrovascular Accident, Infarct)).

INTRACRANIAL NEOPLASTIC AND NONNEOPLASTIC MASS LESIONS

Numerous intracranial masses have been described in dogs and cats. They can be characterized by number, origin, location, size, margination, signal intensity, homogeneity, contrast enhancement, and concurrent imaging findings (eg, ventriculomegaly, changes associated with cranium or meninges, hemorrhage, mineralization, mass effect, edema, cystic or necrotic component).[66,108–112] Mass lesions can be subdivided based on location into intra-axial (arising from within the brain axis) and extra-axial.

Malformations, Hamartomas, Cysts, Borderline Tumors, and Tumorlike Lesions

A variety of conditions is included in this group,[50] and overlap exists with disorders described as congenital malformations and cerebrovascular disease. Cystic lesions

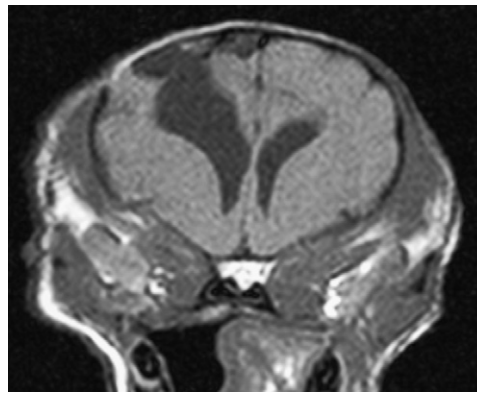

Fig. 9. Transverse T1-W image demonstrating skull fractures and hydrocephalus ex vacuo in an 8-year-old Pomeranian following presumed trauma.

of the brain (eg, arachnoid cysts, ependymal cysts, dermoid and epidermoid cysts) are discussed in the companion article elsewhere in this issue, and congenital disorders of intracranial vessels are discussed in the section on Intracranial Aneurysms and Cerebrovascular Malformations.

Hamartomas are masses formed by disorderly overgrowth of tissue elements normally present at that site.[50] MRI examination in a cat with cerebellar vascular hamartoma showed a heterogeneously T2 hyperintense mass lesion with heterogeneous contrast enhancement.[113]

Hemangiomas are borderline tumors with unclear distinction between hamartoma, malformation, and neoplasia.[50] MRI in a 13-month-old golden retriever with cerebral cavernous hemangioma revealed a large, contrast-enhancing, space-occupying cerebral mass.[114]

Meningioangiomatosis is a rare benign lesion characterized by proliferation of meningothelial cells surrounding small blood vessels.[50] MR examination in a 2-year-old Alaskan malamute showed a large T2 hyperintense mass associated with the cerebrum.[115]

Cholesterol granulomas due to progressive cholesterol accumulation in choroid plexuses are most commonly reported in horses.[50] MRI findings have been described in a cat.[116] An extensive, heterogeneous, space-occupying lesion was found in the area of the falx cerebri, extending from the olfactory bulbs to the tentorium cerebelli, with compression of both hemispheres and thalamus. The mass was mostly hyperintense on STIR, FLAIR, and T2-W images, and hypointense on T1-W images, with heterogeneous contrast enhancement. A peripheral hypointense rim was noted on all sequences, attributed to mineralization, hemorrhage, or cholesterol.

MR diagnosis of intracranial extension of a large nasal mucocele has been reported in a dog.[117] The mass was multilobulated and sharply marginated, hyperintense on T2-W and FLAIR images, isointense on T1-W images, with peripheral ring enhancement. Concurrent findings included mass effect and brain edema.

Meningeal Tumors

Meningiomas originate from the meningeal lining of the brain and are the most common brain tumors in dogs and cats.[110,118] They are typically single lesions, but multiple tumors may occasionally be found.[119] Meningiomas are typically in broad-based contact with underlying bone, have round/ovoid or plaquelike shape, are smoothly marginated, show expansile rather than infiltrative growth pattern, are hypointense to isointense on T1-W images, hyperintense on T2-W/FLAIR images, and show strong and homogeneous to heterogeneous contrast enhancement (**Fig. 10**).[66,108–110,118] Mineralization may be present, which is best demonstrated on T2*-W images. Possible concurrent findings include hyperostosis or pressure atrophy of adjacent bone, brain edema, and mass effect.[112,120] A ''dural tail sign'' (thickening and enhancement of the dura adjacent to an extra-axial mass) is frequently present and is strongly suggestive of meningioma.[121] Cystic meningiomas have been described and predominantly occur in the rostral cranial fossa.[122]

Other tumor types such as disseminated histiocytic sarcoma,[123] lymphoma,[110] granular cell tumor,[124] or metastases (meningeal carcinomatosis)[125] can affect the meninges and have variable appearance on MRI.

Glial Tumors

Glial tumors typically appear as single lesions. Astrocytomas are variable in appearance, with shapes ranging from an ovoid or amorphous mass to a diffuse infiltrate, with distinct to poorly defined margins.[66,108–110,112,126] Leptomeningeal involvement has been reported.[127] Lesions are hypointense to isointense on T1-W, and hyperintense

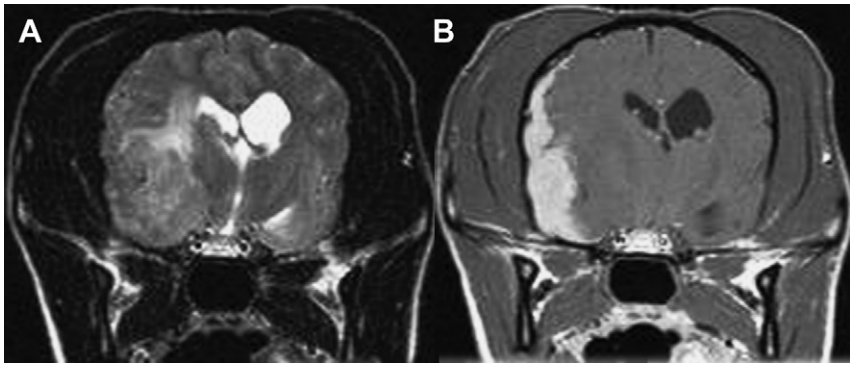

Fig. 10. Plaquelike meningioma in a dog. T2-W (*A*) and postcontrast T1-W (*B*) transverse images demonstrate a mass lesion extending along right temporal and parietal bone that is heterogeneously T2 hyperintense and shows strong homogeneous contrast enhancement. Edema is noted along the white-matter tracts. Deviation of the falx cerebri and compression of the right lateral ventricle are consistent with mass effect. Linear enhancement is noted at the periphery of the mass ("dural tail" sign).

on T2-W images, with contrast enhancement ranging from none to strong, with uniform, nonuniform, and ring-enhancing patterns. Concurrent brain edema is commonly seen.

MRI features of glioblastoma multiforme include heterogeneous increased T2 signal intensity with iso- to hypointense T1-W signal, sharp borders, necrosis, and peritumoral edema (**Fig. 11**).[128] Cyst formation is possible. Irregular margins and a pedunculated shape have been reported in 1 dog.[112] Ring enhancement is commonly seen.

Oligodendrogliomas appear as ovoid, indistinct, smooth to irregular masses, which are hypointense on T1-W and hyperintense on T2-W images, and are typically ring enhancing.[66,109,129,130] Concurrent edema is uncommon. Associated hemorrhage is common.[112]

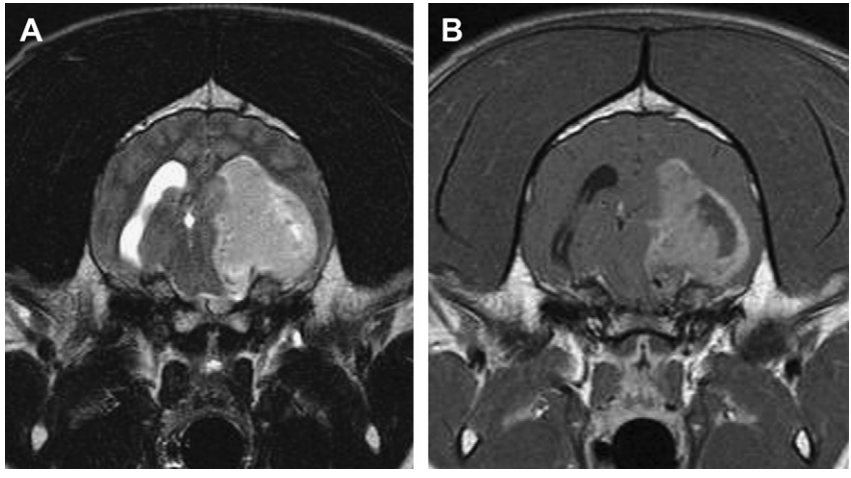

Fig. 11. Glioblastoma multiforme in a 2-year-old golden retriever. T2-W (*A*) and postcontrast T1-W (*B*) transverse images show a heterogeneously T2 hyperintense and inhomogeneously enhancing intra-axial mass with minimal mass effect and invasion of the left lateral ventricle.

Gliomatosis cerebri is a rare, tumorlike disease of glial cells, characterized by diffuse, widespread infiltration, with preservation of brain structures. MRI in a 9-year-old flat-coated retriever demonstrated ill-defined T2/FLAIR hyperintense non-contrast-enhancing areas associated with cerebral hemispheres, brainstem, and cerebellum.[131]

Ventricular Tumors

Choroid plexus tumors originate from the choroid plexus located within the ventricular system, and predominantly occur in the third and fourth ventricle. Choroid plexus papillomas (CPP) and choroid plexus carcinomas (CPC) are predominantly isointense to hyperintense on T1-W and T2-W images, typically with intense and homogeneous contrast enhancement (**Fig. 12**).[108,132] Signal heterogeneity can be observed secondary to cyst formation,[125] mineralization, hemorrhage, or necrosis. The most important feature in differentiating different tumor types is evidence of intraventricular or subarachnoid metastases detected in 35% of CPC but not in CPP.[132] Concurrent ventriculomegaly, perilesional, and periventricular edema are common.

Ependymal tumors (ependymomas) are derived from the lining epithelium of the ventricles and are uncommon in animals.[50] On MRI, ependymomas manifest as well-circumscribed smooth or lobulated tumors associated with the ventricular system. They are isointense on T1-W and hyperintense on T2-W images, show strong contrast enhancement, and are typically associated with hydrocephalus.[66,109,133]

Supraventricular location of meningiomas is common in cats, particularly involving the tela choroidea.[50] They are characterized by smooth margination, homogeneous contrast enhancement, and frequent hydrocephalus.

Primitive Neuroectodermal Tumors and Medulloblastomas

Primitive neuroectodermal tumors (PNETs) are a group of poorly differentiated neoplasms derived from primitive neuroectodermal cells.[50] MR findings in a dog with intracranial PNET include an ill-defined intra-axial mass, involving nasal sinus and frontal lobe, which was hypointense to isointense on T1-W images, hyperintense on T2-W images, and showed moderate to strong heterogeneous contrast enhancement.[112]

Medulloblastomas are malignant tumors occurring in young animals, which are almost exclusively located in the cerebellum.[50] On MRI, a medulloblastoma appears

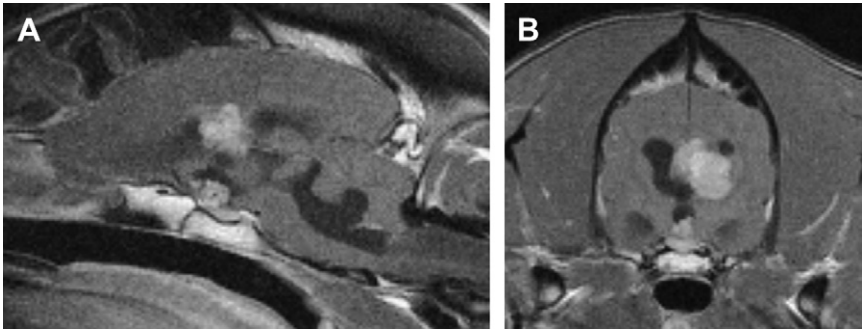

Fig. 12. CPC in a 4-year-old Labrador retriever. Sagittal (*A*) and transverse (*B*) postcontrast T1-W images show an irregularly marginated, strongly contrast-enhancing mass associated with the third ventricle and extending into the left lateral ventricle, with associated hydrocephalus. An additional smaller mass is observed associated with the third ventricle cranial and dorsal to the pituitary gland, which likely represents a metastasis.

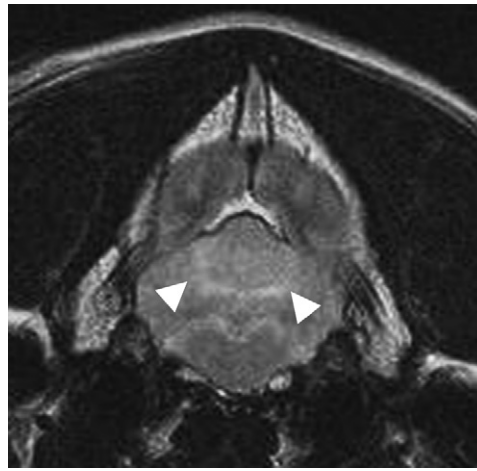

Fig. 13. Medulloblastoma in a 3-year-old mixed breed dog. Transverse FLAIR image shows indistinct T2 hyperintensity associated with the cerebellar vermis (*arrowheads*). No additional abnormalities were detected on other MR sequences.

as a heterogeneous cerebellar mass that is predominantly isointense to hypointense on T1-W images, hyperintense on T2-W images, and shows mild to strong contrast enhancement (**Fig. 13**).[134–136] Concurrent hemorrhage or cysts are possible.

Other CNS Tumors

MR findings have been reported in CNS lymphoma in dogs[112] and cats,[110] and disseminated histiocytic sarcoma in dogs.[112,123,137] Lesions can appear as ill- or well-defined, single or multifocal, intra-axial or extra-axial masses. These are typically isointense to hypointense on T1-W images and hyperintense on T2-W images, show moderate to strong contrast enhancement, and may be associated with edema and mass effect (**Fig. 14**). In cats with extra-axial lymphoma and dogs with extra-axial

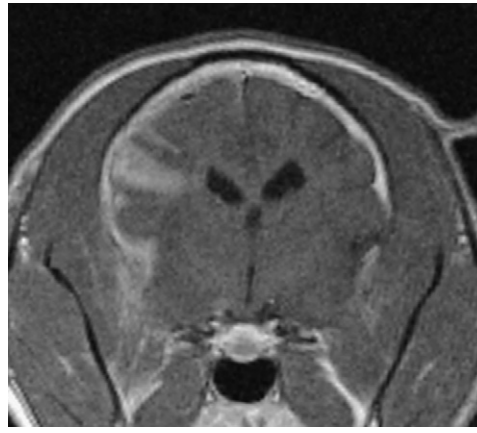

Fig. 14. Disseminated histiocytic sarcoma of the brain in an 11-year-old Norwich terrier. Transverse T1-W postcontrast image shows extensive meningeal and multifocal parenchymal enhancement of the right parietal and temporal lobes. (*Courtesy of* Dr Andrea Matthews, University of Tennessee, USA).

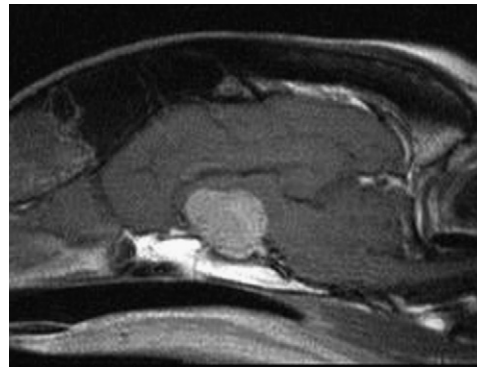

Fig. 15. Pituitary macroadenoma in a dog. Sagittal T1-W postcontrast image shows a smoothly marginated, homogeneously enhancing mass extending dorsally from the pituitary fossa.

histiocytic sarcoma, a "dural tail sign" has been reported after contrast medium administration,[110,123] mimicking a common finding in meningiomas.

Granular cell tumor is a descriptive term for a heterogeneous group of tumors. Intracranial granular cell tumors can be intra- or extra-axial, are typically hyperintense on T2-W images, and show strong contrast enhancement.[124,138,139] Concurrent finding include mass effect, transcalvarial extension, and meningeal enhancement.

CNS-associated Tumors

Pituitary tumors are characterized by their typical position in the pituitary fossa, which is best demonstrated on sagittal images (**Fig. 15**).[66,108,109,140] Pituitary microadenomas may not be readily apparent on conventional MR sequences,[141] and dynamic studies or specific thin-slice sections might be necessary to establish a diagnosis. Pituitary macroadenomas usually appear as well-circumscribed expansile T1 iso- to hypointense and T2/FLAIR hyperintense masses with strong contrast enhancement.

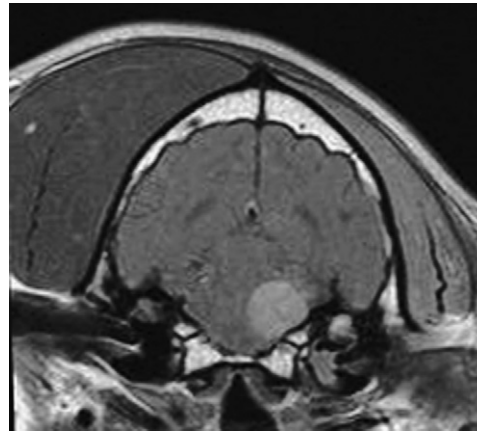

Fig. 16. Trigeminal nerve sheath tumor in a 6-year-old Labrador retriever. Transverse T1-W postcontrast image demonstrates a rounded, smoothly marginated, contrast-enhancing mass associated with the left brainstem. There is atrophy of the left temporalis and masseter muscles. A small amount of material isointense to soft tissue is present within the left tympanic bulla.

Pituitary hemorrhage may occur, resulting in susceptibility artifacts on gradient recalled echo (GRE) T2*-W images and alteration of signal intensity of the mass on pre- and postcontrast images. Pituitary carcinomas show more invasive growth than adenomas, and may invade adjacent basisphenoid bone and pharynx. They are typically inhomogeneous and show nonuniform contrast enhancement.

Craniopharyngiomas originate from remnants of the craniopharyngeal duct ectoderm, which are located above the sella turcica and, by expansion, compress the pituitary gland, optic chiasma, and hypothalamus.[50] MRI examination in 2 cats revealed large masses at the skull base, with extensive bone lysis and cerebral displacement.[142]

Trigeminal nerve sheath tumors are not uncommon in dogs.[50] MRI features include an extra-axial solitary or lobulated mass in the middle or caudal fossa which is typically isointense on T1-W images, isointense or hyperintense on T2-W images, and shows contrast enhancement (**Fig. 16**).[44,143] Atrophy of the temporalis and masseter muscles with increase in signal intensity of these muscles on T1-W images is typically present. Possible additional findings include distortion of the adjacent brain stem and enlarged skull foramina.

Nasal tumors (eg, adenocarcinoma, squamous cell carcinoma, chondrosarcoma, neuroesthesioblastoma) may invade the brain through the cribriform plate. Imaging findings include nasal masses of variable size, intensity, and contrast enhancement, with destruction of cribriform plate and intracranial extension of nasal mass. Cystic/necrotic areas associated with the tumor, and brain edema, are frequently present (**Fig. 17**).[110,144–147]

Tumors of the skull, such as multilobular osteochondrosarcoma or masses originating from adjacent structures, may also extend into the cranial vault.[148]

Metastatic CNS Tumors

Many primary tumors, including hemangiosarcomas and carcinomas, have the potential for wide dissemination, including spread to the CNS.[50,111] Metastases can appear

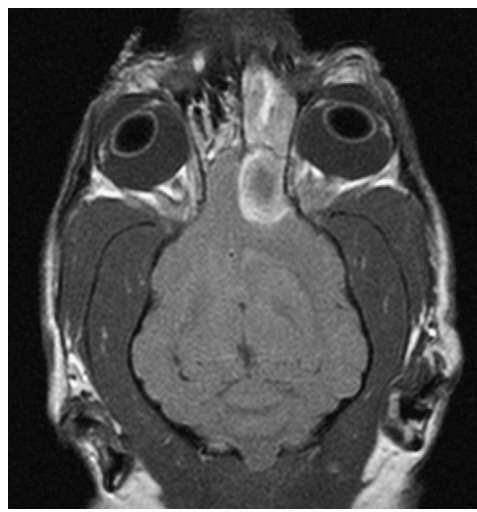

Fig. 17. Nasal squamous cell carcinoma in a 10-year-old miniature pinscher. Dorsal postcontrast T1-W image shows a heterogeneously enhancing mass within the left nasal cavity, with turbinate destruction and invasion of the olfactory bulb through the cribriform plate.

as single or multiple lesions associated with brain parenchyma or meninges, often with associated brain edema. They are commonly rounded to ovoid, appear iso- to hypointense on T1-W images, and hyperintense on T2-W images.[66] Hemangiosarcoma metastases may be associated with hemorrhage. Strong and homogeneous or ring enhancement are commonly noted.

REFERENCES

1. Thomas WB. Nonneoplastic disorders of the brain. Clin Tech Small Anim Pract 1999;14(3):125–47.
2. Bohn AA, Wills TB, West CL, et al. Cerebrospinal fluid analysis and magnetic resonance imaging in the diagnosis of neurologic disease in dogs: a retrospective study. Vet Clin Pathol 2006;35(3):315–20.
3. Lamb CR, Croson PJ, Cappello R, et al. Magnetic resonance imaging findings in 25 dogs with inflammatory cerebrospinal fluid. Vet Radiol Ultrasound 2005;46(1): 17–22.
4. Negrin A, Lamb CR, Cappello R, et al. Results of magnetic resonance imaging in 14 cats with meningoencephalitis. J Feline Med Surg 2007;9(2):109–16.
5. Cherubini GB, Platt SR, Howson S, et al. Comparison of magnetic resonance imaging sequences in dogs with multi-focal intracranial disease. J Small Anim Pract 2008;49(12):634–40.
6. Mellema LM, Samii VF, Vernau KM, et al. Meningeal enhancement on magnetic resonance imaging in 15 dogs and 3 cats. Vet Radiol Ultrasound 2002;43(1): 10–5.
7. Bathen-Noethen A, Stein VM, Puff C, et al. Magnetic resonance imaging findings in acute canine distemper virus infection. J Small Anim Pract 2008;49(9):460–7.
8. Griffin JF, Young BD, Levine JM. Imaging diagnosis - canine chronic distemper meningoencephalitis. Vet Radiol Ultrasound 2009;50(2):182–4.
9. Foley JE, Lapointe JM, Koblik P, et al. Diagnostic features of clinical neurologic feline infectious peritonitis. J Vet Intern Med 1998;12(6):415–23.
10. Braund KG. Inflammatory diseases of the central nervous system. In: Braund KG, editor. Clinical neurology in small animals – localization, diagnosis and treatment. Ithaca (NY): International Veterinary Information Service; 2003. p. 1–45.
11. Mateo I, Lorenzo V, Munoz A, et al. Brainstem abscess due to plant foreign body in a dog. J Vet Intern Med 2007;21(3):535–8.
12. Smith PM, Haughland SP, Jeffery ND. Brain abscess in a dog immunosuppressed using cyclosporin. Vet J 2007;173(3):675–8.
13. Bach JF, Mahony OM, Tidwell AS, et al. Brain abscess and bacterial endocarditis in a Kerry Blue Terrier with a history of immune-mediated thrombocytopenia. J Vet Emerg Critl Care 2007;17(4):409–15.
14. Barrs VR, Nicoll RG, Churcher RK, et al. Intracranial empyema: literature review and two novel cases in cats. J Small Anim Pract 2007;48(8):449–54.
15. Sturges BK, Dickinson PJ, Kortz GD, et al. Clinical signs, magnetic resonance imaging features, and outcome after surgical and medical treatment of otogenic intracranial infection in 11 cats and 4 dogs. J Vet Intern Med 2006;20(3):648–56.
16. Seiler G, Cizinauskas S, Scheidegger J, et al. Low-field magnetic resonance imaging of a pyocephalus and a suspected brain abscess in a German Shepherd dog. Vet Radiol Ultrasound 2001;42(5):417–22.
17. Lavely J, Lipsitz D. Fungal infections of the central nervous system in the dog and cat. Clin Tech Small Anim Pract 2005;20(4):212–9.

18. Stevenson TL, Dickinson PJ, Sturges BK, et al. Magnetic resonance imaging of intracranial cryptococcosis in dogs and cats. Proceedings. Minneapolis (MN): ACVIM June 9–12, 2004.
19. Foster SF, Charles JA, Parker G, et al. Cerebral cryptococcal granuloma in a cat. J Feline Med Surg 2001;3(1):39–44.
20. O'Toole TE, Sato AF, Rozanski EA. Cryptococcosis of the central nervous system in a dog. J Am Vet Med Assoc 2003;222(12):1722–5.
21. Windsor RC, Sturges BK, Vernau KM, et al. Cerebrospinal fluid eosinophilia in dogs. J Vet Intern Med 2009;23(2):275–81.
22. Anor S, Sturges BK, Lafranco L, et al. Systemic phaeohyphomycosis (*Cladophialophora bantiana*) in a dog – clinical diagnosis with stereotactic computed tomographic-guided brain biopsy. J Vet Intern Med 2001;15(3):257–61.
23. Hecht S, Adams WH, Smith JR, et al. CT and MRI findings in intracranial fungal disease in dogs and cats. Proceedings 15th Congress of the International Veterinary Radiology Association. Buzios (Brazil): July 26–31, 2009.
24. Dewey CW. Encephalopathies: disorders of the brain. In: Dewey CW, editor. A practical guide to canine and feline neurology. Ames (IA): Iowa State Press; 2003. p. 99–178.
25. Garosi LS, Platt SR, McConnell JF, et al. Intracranial haemorrhage associated with *Angiostrongylus vasorum* infection in three dogs. J Small Anim Pract 2005;46(2):93–9.
26. Negrin A, Cherubini GB, Steeves E. *Angiostrongylus vasorum* causing meningitis and detection of parasite larvae in the cerebrospinal fluid of a pug dog. J Small Anim Pract 2008;49(9):468–71.
27. Wessmann A, Lu D, Lamb CR, et al. Brain and spinal cord haemorrhages associated with *Angiostrongylus vasorum* infection in four dogs. Vet Rec 2006; 158(25):858–63.
28. Higginbotham MJ, Kent M, Glass EN. Noninfectious inflammatory central nervous system diseases in dogs. Compend Contin Educ Vet 2007;29(8):488–97.
29. Braund KG. Granulomatous meningoencephalomyelitis. J Am Vet Med Assoc 1985;186(2):138–41.
30. Cherubini GB, Platt SR, Anderson TJ, et al. Characteristics of magnetic resonance images of granulomatous meningoencephalomyelitis in 11 dogs. Vet Rec 2006;159(4):110–5.
31. Kitagawa M, Kanayama K, Satoh T, et al. Cerebellar focal granulomatous meningoencephalitis in a dog: clinical findings and MR imaging. J Vet Med A Physiol Pathol Clin Med 2004;51(6):277–9.
32. Lobetti RG, Pearson J. Magnetic resonance imaging in the diagnosis of focal granulomatous meningoencephalitis in two dogs. Vet Radiol Ultrasound 1996; 37(6):424–7.
33. Cordy DR, Holliday TA. A necrotizing meningoencephalitis of pug dogs. Vet Pathol 1989;26(3):191–4.
34. Stalis IH, Chadwick B, Dayrell-Hart B, et al. Necrotizing meningoencephalitis of Maltese dogs. Vet Pathol 1995;32(3):230–5.
35. Higgins RJ, Dickinson PJ, Kube SA, et al. Necrotizing meningoencephalitis in five Chihuahua dogs. Vet Pathol 2008;45(3):336–46.
36. Cantile C, Chianini F, Arispici M, et al. Necrotizing meningoencephalitis associated with cortical hippocampal hamartia in a Pekingese dog. Vet Pathol 2001; 38(1):119–22.
37. Timmann D, Konar M, Howard J, et al. Necrotising encephalitis in a French bulldog. J Small Anim Pract 2007;48(6):339–42.

38. Flegel T, Henke D, Boettcher IC, et al. Magnetic resonance imaging findings in histologically confirmed Pug dog encephalitis. Vet Radiol Ultrasound 2008; 49(5):419–24.
39. Jull BA, Merryman JI, Thomas WB, et al. Necrotizing encephalitis in a Yorkshire terrier. J Am Vet Med Assoc 1997;211(8):1005–7.
40. Lotti D, Capucchio MT, Gaidolfi E, et al. Necrotizing encephalitis in a Yorkshire terrier: clinical, imaging, and pathologic findings. Vet Radiol Ultrasound 1999; 40(6):622–6.
41. Sawashima Y, Sawashima K, Taura Y, et al. Clinical and pathological findings of a Yorkshire terrier affected with necrotizing encephalitis. J Vet Med Sci 1996; 58(7):659–61.
42. von Praun F, Matiasek K, Grevel V, et al. Magnetic resonance imaging and pathologic findings associated with necrotizing encephalitis in two Yorkshire terriers. Vet Radiol Ultrasound 2006;47(3):260–4.
43. Kuwabara M, Tanaka S, Fujiwara K. Magnetic resonance imaging and histopathology of encephalitis in a Pug. J Vet Med Sci 1998;60(12):1353–5.
44. Schultz RM, Tucker RL, Gavin PR, et al. Magnetic resonance imaging of acquired trigeminal nerve disorders in six dogs. Vet Radiol Ultrasound 2007; 48(2):101–4.
45. National Institute of Neurological Disorders and Stroke. Special report from the National Institute of Neurological Disorders and Stroke. Classification of cerebrovascular diseases III. Stroke 1990;21(4):637–76.
46. Terbrugge KG, Rao KCVG. Intracranial aneurysms and vascular malformations. In: Lee SH, Rao KCVG, Zimmerman RA, editors. Cranial MRI and CT. 4th edition. New York: McGraw-Hill; 1999. p. 517–56.
47. Ozsarlak O, Van Goethem JW, Maes M, et al. MR angiography of the intracranial vessels: technical aspects and clinical applications. Neuroradiology 2004; 46(12):955–72.
48. Tidwell AS, Ross LA, Kleine LJ. Computed tomography and magnetic resonance imaging of cavernous sinus enlargement in a dog with unilateral exophthalmos. Vet Radiol Ultrasound 1997;38(5):363–70.
49. McCormick WF. Pathology of vascular malformations of the brain. In: Wilson CB, Stein BM, editors. Intracranial arteriovenous malformations of the brain. Baltimore (MD): Williams and Wilkins; 1984. p. 44–63.
50. Summers BA, Cummings JF, de Lahunta A. Veterinary neuropathology. St. Louis (MO): Mosby; 1995.
51. Joseph RJ, Greenlee PG, Carrillo JM, et al. Canine cerebrovascular disease. Findings in 17 cases. J Am Anim Hosp Assoc 1988;24:569–76.
52. Irwin JC, Dewey CW, Stefanacci JD. Suspected cerebellar infarcts in 4 dogs. J Vet Emerg Critl Care 2007;17(3):268–74.
53. Garosi L, McConnell JE, Platt SR, et al. Results of diagnostic investigations and long-term outcome of 33 dogs with brain infarction (2000–2004). J Vet Intern Med 2005;19(5):725–31.
54. Kent M, Delahunta A, Tidwell AS. MR imaging findings in a dog with intravascular lymphoma in the brain. Vet Radiol Ultrasound 2001;42(6):504–10.
55. Bush WW, Throop JL, McManus PM, et al. Intravascular lymphoma involving the central and peripheral nervous systems in a dog. J Am Anim Hosp Assoc 2003; 39(1):90–6.
56. Cachin M, Vandevelde M. Cerebral infarction associated with septic thromboemboli in the dog. Proceedings 8th Annual Meeting of the Veterinary Medicine Forum. Washington, DC: May 10, 1990.

57. Axlund TW, Isaacs AM, Holland M, et al. Fibrocartilaginous embolic encephalomyelopathy of the brainstem and midcervical spinal cord in a dog. J Vet Intern Med 2004;18(5):765–7.
58. Kotani T, Tomimura T, Ogura M, et al. Cerebral infarction caused by *Dirofilaria immitis* in three dogs. Jpn J Vet Sci 1975;37:379–90.
59. Kalimo H, Kaste M, Haltia M. Vascular diseases. In: Graham DI, Lantos PL, editors. Greenfield's neuropathology. 7th edition. London: Arnold; 2002. p. 233–80.
60. McConnell JF, Garosi L, Platt SR. Magnetic resonance imaging findings of presumed cerebellar cerebrovascular accident in twelve dogs. Vet Radiol Ultrasound 2005;46(1):1–10.
61. Schellinger PD, Fiebach JB, Hacke W. Imaging-based decision making in thrombolytic therapy for ischemic stroke: present status. Stroke 2003;34(2):575–83.
62. Crawley AP, Poublanc J, Ferrari P, et al. Basics of diffusion and perfusion MRI. Appl Radiol 2003;32(4):13–23.
63. Thomas WB, Sorjonen DC, Scheuler RO, et al. Magnetic resonance imaging of brain infarction in seven dogs. Vet Radiol Ultrasound 1996;37(5):345–50.
64. Garosi L, McConnell JF, Platt SR, et al. Clinical and topographic magnetic resonance characteristics of suspected brain infarction in 40 dogs. J Vet Intern Med 2006;20(2):311–21.
65. Garosi LS, McConnell JF. Ischaemic stroke in dogs and humans: a comparative review. J Small Anim Pract 2005;46(11):521–9.
66. Kraft SL, Gavin PR. Intracranial neoplasia. Clin Tech Small Anim Pract 1999; 14(2):112–23.
67. Whitley NT, Corzo-Menendez N, Carmichael NG, et al. Cerebral and conjunctival haemorrhages associated with von Willebrand factor deficiency and canine angiostrongylosis. J Small Anim Pract 2005;46(2):75–8.
68. Bradley WG Jr. MR appearance of hemorrhage in the brain. Radiology 1993; 189(1):15–26.
69. Parizel PM, Makkat S, Van Miert E, et al. Intracranial hemorrhage: principles of CT and MRI interpretation. Eur Radiol 2001;11(9):1770–83.
70. Liang L, Korogi Y, Sugahara T, et al. Detection of intracranial hemorrhage with susceptibility-weighted MR sequences. Am J Neuroradiol 1999;20(8):1527–34.
71. Tidwell AS. Principles of computed tomography and magnetic resonance imaging. In: Thrall DE, editor. Textbook of veterinary diagnostic radiology. 5th edition. St. Louis (MO): Saunders Elsevier; 2007. p. 50–77.
72. Anzalone N, Scotti R, Riva R. Neuroradiologic differential diagnosis of cerebral intraparenchymal hemorrhage. Neurol Sci 2004;25(Suppl 1):S3–5.
73. Williams KJ, Summers BA, de Lahunta A. Cerebrospinal cuterebriasis in cats and its association with feline ischemic encephalopathy. Vet Pathol 1998; 35(5):330–43.
74. Quesnel AD, Parent JM, McDonell W, et al. Diagnostic evaluation of cats with seizure disorders: 30 cases (1991–1993). J Am Vet Med Assoc 1997;210(1): 65–71.
75. White BC, Grossman LI, O'Neil BJ, et al. Global brain ischemia and reperfusion. Ann Emerg Med 1996;27(5):588–94.
76. Timm K, Flegel T, Oechtering G. Sequential magnetic resonance imaging changes after suspected global brain ischaemia in a dog. J Small Anim Pract 2008;49(8):408–12.
77. Panarello GP, Dewey CW, Baroni G, et al. Magnetic resonance imaging of two suspected cases of global brain ischemia. J Vet Emerg Critl Care 2004;14(4): 269–77.

78. Wenger DA, Victoria T, Rafi MA, et al. Globoid cell leukodystrophy in cairn and West Highland white terriers. J Hered 1999;90(1):138–42.
79. Cozzi F, Vite CH, Wenger DA, et al. MRI and electrophysiological abnormalities in a case of canine globoid cell leucodystrophy. J Small Anim Pract 1998;39(8): 401–5.
80. Matsuki N, Yamato O, Kusuda M, et al. Magnetic resonance imaging of GM2-gangliosidosis in a golden retriever. Can Vet J 2005;46(3):275–8.
81. Kaye EM, Alroy J, Raghavan SS, et al. Dysmyelinogenesis in animal model of GM1 gangliosidosis. Pediatr Neurol 1992;8(4):255–61.
82. Koie H, Shibuya H, Sato T, et al. Magnetic resonance imaging of neuronal ceroid lipofuscinosis in a border collie. J Vet Med Sci 2004;66(11):1453–6.
83. Armstrong D, Quisling RG, Webb A, et al. Computed tomographic and nuclear magnetic resonance correlation of canine ceroid-lipofuscinosis with aging. Neurobiol Aging 1983;4(4):297–303.
84. Vite CH, Magnitsky S, Aleman D, et al. Apparent diffusion coefficient reveals gray and white matter disease, and T2 mapping detects white matter disease in the brain in feline alpha-mannosidosis. Am J Neuroradiol 2008; 29(2):308–13.
85. Vite CH, McGowan JC, Braund KG, et al. Histopathology, electrodiagnostic testing, and magnetic resonance imaging show significant peripheral and central nervous system myelin abnormalities in the cat model of alpha-mannosidosis. J Neuropathol Exp Neurol 2001;60(8):817–28.
86. Ellinwood NM, Wang P, Skeen T, et al. A model of mucopolysaccharidosis IIIB (Sanfilippo syndrome type IIIB): *N*-acetyl-alpha-D-glucosaminidase deficiency in Schipperke dogs. J Inherit Metab Dis 2003;26(5):489–504.
87. Abramson CJ, Platt SR, Jakobs C, et al. L-2-Hydroxyglutaric aciduria in Staffordshire bull terriers. J Vet Intern Med 2003;17(4):551–6.
88. Brenner O, de Lahunta A, Summers BA, et al. Hereditary polioencephalomyelopathy of the Australian cattle dog. Acta Neuropathol 1997;94(1):54–66.
89. Brenner O, Wakshlag JJ, Summers BA, et al. Alaskan husky encephalopathy – a canine neurodegenerative disorder resembling subacute necrotizing encephalomyelopathy (Leigh syndrome). Acta Neuropathol 2000;100(1):50–62.
90. Wakshlag JJ, de Lahunta A, Robinson T, et al. Subacute necrotising encephalopathy in an Alaskan husky. J Small Anim Pract 1999;40(12):585–9.
91. Harkin KR, Goggin JM, DeBey BM, et al. Magnetic resonance imaging of the brain of a dog with hereditary polioencephalomyelopathy. J Am Vet Med Assoc 1999;214(9):1342–4.
92. Torisu S, Washizu M, Hasegawa D, et al. Brain magnetic resonance imaging characteristics in dogs and cats with congenital portosystemic shunts. Vet Radiol Ultrasound 2005;46(6):447–51.
93. Garosi LS, Dennis R, Platt SR, et al. Thiamine deficiency in a dog: clinical, clinicopathologic, and magnetic resonance imaging findings. J Vet Intern Med 2003;17(5):719–23.
94. Singh M, Thompson M, Sullivan N, et al. Thiamine deficiency in dogs due to the feeding of sulphite preserved meat. Aust Vet J 2005;83(7):412–7.
95. Penderis J, McConnell JF, Calvin J. Magnetic resonance imaging features of thiamine deficiency in a cat. Vet Rec 2007;160(8):270–2.
96. Ashrafian H, Davey P. A review of the causes of central pontine myelinosis: yet another apoptotic illness? Eur J Neurol 2001;8(2):103–9.
97. O'Brien DP, Kroll RA, Johnson GC, et al. Myelinolysis after correction of hyponatremia in two dogs. J Vet Intern Med 1994;8(1):40–8.

98. Mariani CL, Clemmons RM, Graham JP, et al. Magnetic resonance imaging of spongy degeneration of the central nervous system in a Labrador retriever. Vet Radiol Ultrasound 2001;42(4):285–90.
99. Tamura S, Tamura Y, Uchida K. Magnetic resonance imaging findings of neuroaxonal dystrophy in a papillon puppy. J Small Anim Pract 2007;48(8): 458–61.
100. Flegel T, Matiasek K, Henke D, et al. Cerebellar cortical degeneration with selective granule cell loss in Bavarian mountain dogs. J Small Anim Pract 2007;48(8): 462–5.
101. Henke D, Bottcher P, Doherr MG, et al. Computer-assisted magnetic resonance imaging brain morphometry in American Staffordshire terriers with cerebellar cortical degeneration. J Vet Intern Med 2008;22(4):969–75.
102. Nibe K, Kita C, Morozumi M, et al. Clinicopathological features of canine neuroaxonal dystrophy and cerebellar cortical abiotrophy in Papillon and Papillon-related dogs. J Vet Med Sci 2007;69(10):1047–52.
103. Olby N, Blot S, Thibaud JL, et al. Cerebellar cortical degeneration in adult American Staffordshire terriers. J Vet Intern Med 2004;18(2):201–8.
104. van der Merwe LL, Lane E. Diagnosis of cerebellar cortical degeneration in a Scottish terrier using magnetic resonance imaging. J Small Anim Pract 2001;42(8):409–12.
105. Olby N, Munana K, De Risio L, et al. Cervical injury following a horse kick to the head in two dogs. J Am Anim Hosp Assoc 2002;38(4):321–6.
106. Adamo PF, Crawford JT, Stepien RL. Subdural hematoma of the brainstem in a dog: magnetic resonance findings and treatment. J Am Anim Hosp Assoc 2005;41(6):400–5.
107. Kitagawa M, Okada M, Kanayama K, et al. Traumatic intracerebral hematoma in a dog: MR images and clinical findings. J Vet Med Sci 2005;67(8):843–6.
108. Thomas WB, Wheeler SJ, Kramer R, et al. Magnetic resonance imaging features of primary brain tumors in dogs. Vet Radiol Ultrasound 1996;37(1):20–7.
109. Kraft SL, Gavin PR, DeHaan C, et al. Retrospective review of 50 canine intracranial tumors evaluated by magnetic resonance imaging. J Vet Intern Med 1997; 11(4):218–25.
110. Troxel MT, Vite CH, Massicotte C, et al. Magnetic resonance imaging features of feline intracranial neoplasia: retrospective analysis of 46 cats. J Vet Intern Med 2004;18(2):176–89.
111. Snyder JM, Lipitz L, Skorupski KA, et al. Secondary intracranial neoplasia in the dog: 177 cases (1986–2003). J Vet Intern Med 2008;22(1):172–7.
112. Snyder JM, Shofer FS, Van Winkle TJ, et al. Canine intracranial primary neoplasia: 173 cases (1986–2003). J Vet Intern Med 2006;20(3):669–75.
113. Stalin CE, Granger N, Jeffery ND. Cerebellar vascular hamartoma in a British shorthair cat. J Feline Med Surg 2008;10(2):206–11.
114. Schoeman JP, Stidworthy MF, Penderis J, et al. Magnetic resonance imaging of a cerebral cavernous haemangioma in a dog. J S Afr Vet Assoc 2002;73(4): 207–10.
115. Lorenzo V, Pumarola M, Munoz A. Meningioangiomatosis in a dog: magnetic resonance imaging and neuropathological studies. J Small Anim Pract 1998; 39(10):486–9.
116. Fluehmann G, Konar M, Jaggy A, et al. Cerebral cholesterol granuloma in a cat. J Vet Intern Med 2006;20(5):1241–4.
117. Sessums KB, Lane SB. Imaging diagnosis: intracranial mucocele in a dog. Vet Radiol Ultrasound 2008;49(6):564–6.

118. Sturges BK, Dickinson PJ, Bollen AW, et al. Magnetic resonance imaging and histological classification of intracranial meningiomas in 112 dogs. J Vet Intern Med 2008;22(3):586–95.
119. Forterre F, Tomek A, Konar M, et al. Multiple meningiomas: clinical, radiological, surgical, and pathological findings with outcome in four cats. J Feline Med Surg 2007;9(1):36–43.
120. Hathcock JT. Low field magnetic resonance imaging characteristics of cranial vault meningiomas in 13 dogs. Vet Radiol Ultrasound 1996;37(4): 257–63.
121. Graham JP, Newell SM, Voges AK, et al. The dural tail sign in the diagnosis of meningiomas. Vet Radiol Ultrasound 1998;39(4):297–302.
122. Johnson LM, Hecht S, Arendse AU, et al. What is your diagnosis? Cystic meningioma. J Am Vet Med Assoc 2007;231(6):861–2.
123. Tamura S, Tamura Y, Nakamoto Y, et al. MR imaging of histiocytic sarcoma of the canine brain. Vet Radiol Ultrasound 2009;50(2):178–81.
124. Sharkey LC, McDonnell JJ, Alroy J. Cytology of a mass on the meningeal surface of the left brain in a dog. Vet Clin Pathol 2004;33(2):111–4.
125. Lipsitz D, Levitski RE, Chauvet AE. Magnetic resonance imaging of a choroid plexus carcinoma and meningeal carcinomatosis in a dog. Vet Radiol Ultrasound 1999;40(3):246–50.
126. Kube SA, Bruyette DS, Hanson SM. Astrocytomas in young dogs. J Am Anim Hosp Assoc 2003;39(3):288–93.
127. Kraft SL, Gavin PR, Leathers CW, et al. Diffuse cerebral and leptomeningeal astrocytoma in dogs: MR features. J Comput Assist Tomogr 1990;14(4):555–60.
128. Lipsitz D, Higgins RJ, Kortz GD, et al. Glioblastoma multiforme: clinical findings, magnetic resonance imaging, and pathology in five dogs. Vet Pathol 2003; 40(6):659–69.
129. Stacy BA, Stevenson TL, Lipsitz D, et al. Simultaneously occurring oligodendroglioma and meningioma in a dog. J Vet Intern Med 2003;17(3):357–9.
130. Dickinson PJ, Keel MK, Higgins RJ, et al. Clinical and pathologic features of oligodendrogliomas in two cats. Vet Pathol 2000;37(2):160–7.
131. Gruber A, Leschnik M, Kneissl S, et al. Gliomatosis cerebri in a dog. J Vet Med A Physiol Pathol Clin Med 2006;53(8):435–8.
132. Westworth DR, Dickinson PJ, Vernau W, et al. Choroid plexus tumors in 56 dogs (1985–2007). J Vet Intern Med 2008;22(5):1157–65.
133. Vural SA, Besalti O, Ilhan F, et al. Ventricular ependymoma in a German Shepherd dog. Vet J 2006;172(1):185–7.
134. MacKillop E, Thrall DE, Ranck RS, et al. Imaging diagnosis – synchronous primary brain tumors in a dog. Vet Radiol Ultrasound 2007;48(6):550–3.
135. McConnell JF, Platt S, Smith KC. Magnetic resonance imaging findings of an intracranial medulloblastoma in a Polish lowland sheepdog. Vet Radiol Ultrasound 2004;45(1):17–22.
136. Kitagawa M, Koie H, Kanayamat K, et al. Medulloblastoma in a cat: clinical and MRI findings. J Small Anim Pract 2003;44(3):139–42.
137. Tzipory L, Vernau KM, Sturges BK, et al. Antemortem diagnosis of localized central nervous system histiocytic sarcoma in 2 dogs. J Vet Intern Med 2009; 23(2):369–74.
138. Higgins RJ, LeCouteur RA, Vernau KM, et al. Granular cell tumor of the canine central nervous system: two cases. Vet Pathol 2001;38(6):620–7.
139. Liu CH, Liu CI, Liang SL, et al. Intracranial granular cell tumor in a dog. J Vet Med Sci 2004;66(1):77–9.

140. Duesberg CA, Feldman EC, Nelson RW, et al. Magnetic resonance imaging for diagnosis of pituitary macrotumors in dogs. J Am Vet Med Assoc 1995;206(5): 657–62.
141. Wood FD, Pollard RE, Uerling MR, et al. Diagnostic imaging findings and endocrine test results in dogs with pituitary-dependent hyperadrenocorticism that did or did not have neurologic abnormalities: 157 cases (1989–2005). J Am Vet Med Assoc 2007;231(7):1081–5.
142. Nagata T, Nakayama H, Uchida K, et al. Two cases of feline malignant craniopharyngioma. Vet Pathol 2005;42(5):663–5.
143. Bagley RS, Wheeler SJ, Klopp L, et al. Clinical features of trigeminal nerve-sheath tumor in 10 dogs. J Am Anim Hosp Assoc 1998;34(1):19–25.
144. Avner A, Dobson JM, Sales JI, et al. Retrospective review of 50 canine nasal tumours evaluated by low-field magnetic resonance imaging. J Small Anim Pract 2008;49(5):233–9.
145. Kitagawa M, Okada M, Yamamura H, et al. Diagnosis of olfactory neuroblastoma in a dog by magnetic resonance imaging. Vet Rec 2006;159(9):288–9.
146. Miles MS, Dhaliwal RS, Moore MP, et al. Association of magnetic resonance imaging findings and histologic diagnosis in dogs with nasal disease: 78 cases (2001–2004). J Am Vet Med Assoc 2008;232(12):1844–9.
147. Moore MP, Gavin PR, Kraft SL, et al. MR, CT and clinical features from four dogs with nasal tumors involving the rostral cerebrum. Vet Radiol 1991;32(1):19–25.
148. Lipsitz D, Levitski RE, Berry WL. Magnetic resonance imaging features of multilobular osteochondrosarcoma in 3 dogs. Vet Radiol Ultrasound 2001;42(1): 14–9.